Mesoscopic ferromagnet-superconductor junctions and the proximity effect

J. Aumentado and V. Chandrasekhar
Department of Physics and Astronomy, Northwestern University, Evanston, Illinois 60208
(Received 9 April 2001; published 3 July 2001)

We have measured the electrical transport of submicron ferromagnets (Ni) in contact with a mesoscopic superconductor (Al) for a range of interface resistances. In the geometry measured, the interface and the ferromagnet are measured separately. The ferromagnet itself shows no appreciable superconducting proximity effect, but the ferromagnet/superconductor interface exhibits strong temperature, field, and current bias dependences. These effects are dependent on the local magnetic field distribution near the interface arising from the ferromagnet. We find that the temperature dependences can be qualitatively described by a modified version of the Blonder-Tinkham-Klapwijk theory for normal-superconductor transport.

DOI: 10.1103/PhysRevB.64.054505 PACS number(s): 74.25.Fy, 73.23.−b, 73.50.−h, 85.30.Hi

There has been much interest recently in the possibility of observing the superconducting proximity effect in a ferromagnetic metal.[1–3] In general, one does not expect to see the proximity effect in a ferromagnet due to the large internal exchange field which is expected to destroy superconducting correlations in the ferromagnet at distances greater than the exchange length l_{ex} (typically a few nanometers for the transition-metal ferromagnets). This point of view has been reinforced by many experiments on ferromagnet/superconductor (FS) multilayers, where it was found that two superconducting layers are effectively decoupled if the thickness of the ferromagnet between them is much greater than l_{ex}.[4,5]

More recently, attention has focused on mesoscopic FS structures, where experimental results seem to indicate that superconducting correlations can penetrate into the ferromagnet at distances much greater than l_{ex}. Giroud *et al.*[6] measured the temperature-dependent resistance of mesoscopic Co rings in contact with a superconducting Al film, and found a small but significant temperature and bias-dependent differential resistance, reminiscent of the reentrant proximity effect observed in normal metal/superconductor (NS) structures. They estimated a penetration of superconducting correlations into the Co to a distance of $\sim$180 nm, much larger than l_{ex}. Lawrence and Giordano[7] measured Ni wires in contact with Sn pads, and observed a large change in resistance which they attributed to a proximity effect that penetrated up to 46 nm into the Ni. Finally, Petrashov *et al.*[8] measured Ni wires in contact with Al films, and observed an anomalously large change in the resistance of the devices below the transition temperature of the superconductor. This change was also reflected in the differential resistance of the devices as a function of dc current below the superconducting transition. They attributed this to a proximity effect which penetrated up to a distance of 600 nm into the ferromagnet, again much larger than l_{ex}.

In all these experiments, the superconductor was measured either in parallel or in series with the ferromagnet. In this paper, we present results of our measurements of the resistance of mesoscopic Ni/Al structures as a function of temperature, dc current, and magnetic field. In contrast to the experiments discussed, the devices have multiple nonmagnetic Au probes which allow us to separately probe the resistance of the ferromagnet, the FS interface, and the Al film. In agreement with previous experiments, we find large changes in resistance below the superconducting transition of the Al. However, the multiprobe nature of our devices allows us to determine that the primary contribution to this resistance change in our samples arises from the FS interface itself, with essentially no contribution from the ferromagnet, indicating the absence of long-range superconducting correlations in the ferromagnet. In addition, we find that the interface resistances of our devices are sensitive to the magnetic state of the ferromagnetic particle. The resistance of the interface can be described qualitatively by the model of Blonder, Tinkham, and Klapwijk (BTK),[9] taking into account the effects of partial spin polarization of the conduction electrons in the ferromagnet.[10,11]

Our samples are fabricated in three separate *e*-beam lithography steps, with the polycrystalline metal films deposited by *e*-gun deposition. Seven different samples were measured, but here we present results on only a few representative samples. Figures 1(a) and 1(b) show a scanning electron micrograph of one of our samples along with a sample schematic. The majority of our devices consist of an elliptical Ni particle in contact with a superconducting Al film.[12] To ensure predictable magnetic behavior, the Ni elements are patterned and deposited first so that they lay flat on the substrate, and the elliptical shape of the Ni particles ensures that the magnetic shape anisotropy aligns the magnetization of the particle in-plane along the major axis of the

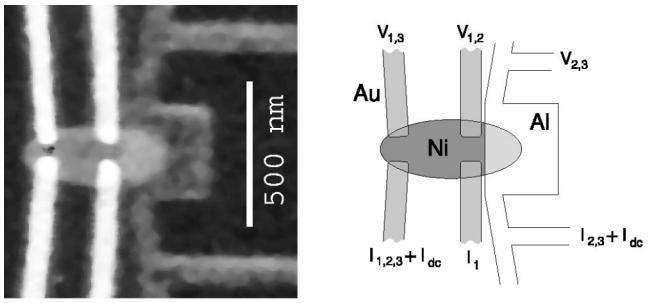

FIG. 1. (a) Micrograph of a typical FS structure. The picture area is scaled to 1×1 μm^2. (b) Schematic of the probe configuration. The various probe configurations are denoted by the subscripts, as referred to in the text.

ellipse.[13] Au wires are then patterned and deposited, contacting the Ni particle and providing nonmagnetic electronic probes with which we can monitor the magnetic behavior of the Ni particle,[13] as well as measure any proximity effect in it independent of the response of the FS interface. In addition, two Au probes are within 20–50 nm of the interface, ensuring that only a very small part of the ferromagnet is included in measurements of the FS interface. The superconducting layer is then deposited in the final lithography step. All interfaces are cleaned using an ac Ar^+ etch prior to the deposition of the Au and Al layers. The thickness of the Ni films is ~30 nm, that of the Al film is ~50–60 nm, and that of the Au electrodes is ~50–60 nm. In addition to the FS samples themselves, control samples of Ni wires, Al wires, and Ni/Al interface samples are also fabricated simultaneously in order to characterize the material parameters of the films and interfaces. From low-temperature measurements on these control samples, the resistivity of the Ni film was estimated to be $\rho_{Ni} \sim 6.6\ \mu\Omega$ cm and that of the Al film $\rho_{Al} \sim 8.4\ \mu\Omega$ cm, corresponding to electronic diffusion constants $D=(1/3)v_F l$ (where v_F is the Fermi velocity, and l is the elastic mean free path) of $D_{Ni} \sim 76$ cm^2/s and $D_{Al} \sim 26$ cm^2/s, respectively.[14]

The measurements are performed at temperatures down to ~260 mK using standard ac lock-in techniques, with all magnetic fields applied *in-plane* along the easy axis of the Ni particles using a superconducting split-coil magnet. The application of such a longitudinal, in-plane magnetic field is advantageous in two respects: first, the critical field of the Al is much greater in this configuration, and second, the magnetization of the elliptical particles lies in-plane and is single domain at remanence.[13] With this geometry, a number of four-probe measurement configurations are possible [see Fig. 1(b)]. In this paper we concentrate on only three (denoted by the subscripts in the figure). Configuration 1 measures the resistance of the Ni particle, configuration 2 measures the interface and a small contribution (20–50 nm) from the Ni between the Ni and Al probes, and configuration 3 measures both the interface and the Ni particle resistance in series, and is equivalent to the probe geometry used in Ref. 8. Measurements which include the interface in the current path are performed with an excitation current of 10–50 nA, while the Ni particle measurements are taken with currents of 100–500 nA, low enough to avoid self-heating.

Figure 2(a) shows the zero-field temperature dependences of the resistances of the FS interface (R_2) and the FS interface in series with the Ni ellipse (R_3). The normal-state resistance of the interface in this device was 23.8 Ω. The magnetic state of the particle was prepared by saturating the magnetization in a magnetic field of +4 kG aligned along the major axis of the elliptical Ni particle, such that it contained no domain structure at remanence. The resistances R_2 and R_3 both display a sharp increase at the superconducting transition, and then decrease until the temperature reaches 0.9 K, below which the resistances begin to rise again. The behavior of R_3 simply duplicates that of the interface R_2, being offset from it by approximately 2 Ω, which corresponds to the resistance of the Ni particle itself. The temperature dependence of R_3 is reminiscent of the reentrant

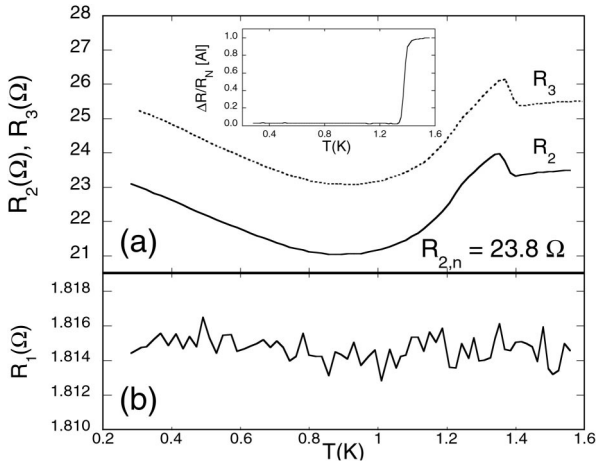

FIG. 2. (a) Temperature dependence of the interface resistance, $R_2=23.8\Omega$, and the interface resistance and Ni ellipse in series, R_3. Inset: the resistance of the overlapping Al wire, R_{Al}. (b) The resistance of the Ni ellipse, R_1.

proximity effect seen in normal metal mesoscopic structures in contact with superconductors,[15] and, if one had access to these data alone, one might conclude that the ferromagnet exhibits a strong superconducting proximity effect. However, a similar resistance change is *not* seen in the Ni particle by itself [R_1 in Fig. 2(b)], indicating that the resistance change arises in the region of the sample between the voltage probes of configuration 2, i.e., at the FS interface. Similar behavior is also observed in our other samples with barrier resistances ranging from 19 Ω to 1.3 MΩ. We therefore conclude that *no long-range superconducting coherence effects are present in the ferromagnet in our samples.*

The peak in the resistance observed near the superconducting transition in Fig. 2(a) is similar to that observed in other mesoscopic superconducting samples, and is associated with charge imbalance effects in the Al films.[16] Below the resistance peak, the data can be qualitatively described by the BTK theory, with suitable modifications to account for spin polarization as we describe below.

The normalized conductance of an NS point contact in the BTK model is[9]

$$g(Z,T)=(1+Z^2)\int_{-\infty}^{+\infty}\left(-\frac{\partial f_0}{\partial E}\right)[1+A(E)-B(E)]dE, \tag{1}$$

where f_0 is the Fermi function, and $A(E)$ and $B(E)$ are the BTK parameters which describe Andreev and normal reflection processes, respectively. $A(E)$ and $B(E)$ depend on the gap in the superconductor Δ and the BTK parameter Z, which parametrizes the strength of the interface. In the case when the normal metal is a ferromagnet (FS transport), the spin polarization $P=[N_\uparrow(E_F)-N_\downarrow(E_F)]/[N_\uparrow(E_F)+N_\downarrow(E_F)]$ of the electrons in the ferromagnet must be considered. Since Andreev reflection processes can only occur between pairs of spin-up and spin-down electrons, the fraction of the electrons that can participate in such a process is $(1-P)$ of the total population. To account for this in the BTK model,[9] one may replace the factor $A(E)$ in Eq. (1)

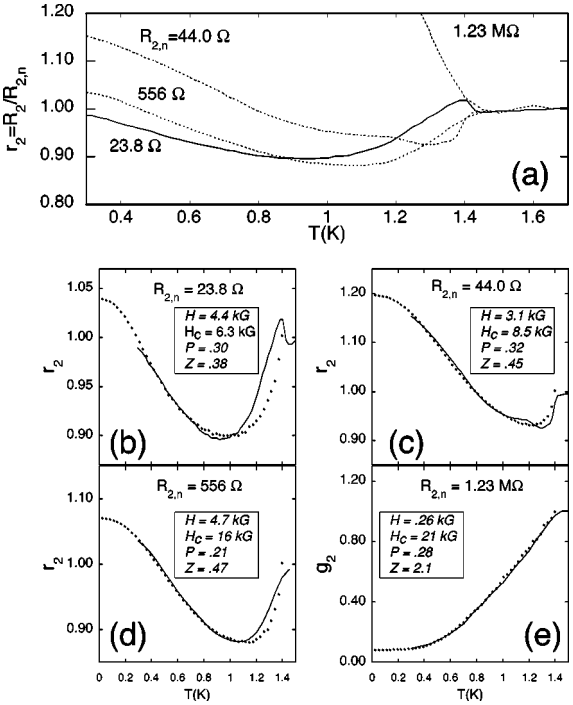

FIG. 3. (a) Normalized experimental temperature dependences for various values of the normal-state barrier resistance, $R_{2,n}$. (b) The lowest resistance device (solid trace) shows a charge imbalance peak near $T_c(=1.4\ \mathrm{K})$. (b)–(e) BTK fits (points) for various values of the interface resistance, $R_{2,n}$. Our experimental data are shown as the solid traces. Inset: Fitting parameters. Free parameters appear in italics [(b)–(d) normalized resistances, (e) normalized conductance].

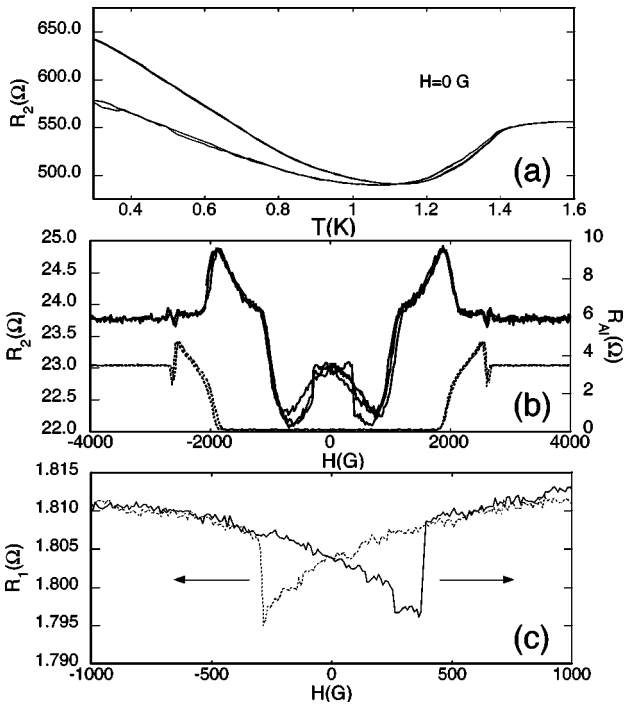

FIG. 4. (a) Multiple states in the temperature dependence of the 556-Ω interface resistance sample. (b) Magnetoresistances (MR's) (at $T=300$ mK) of the Al/Ni interface $R_2(H)$ showing multiple states (left axis, solid trace) and the overlapping Al wire, $R_{Al}(H)$ (right axis, dashed trace). (c) MR (at $T=300$ mK) of the Ni ellipse, $R_1(H)$ (arrows indicate sweep direction). Note: H is the externally applied field.

with $A'(E)=(1-P)A(E)$.[10,11] This substitution was performed by Soulen *et al.*[10,11] to determine the polarization of various ferromagnetic metals using point-contact spectroscopy in clean contacts. Using this same substitution, one may fit the temperature dependence for arbitrary values of Z and P. Finally, the presence of a finite field on the superconductor, which is the sum of any externally applied field and the field due to the magnetization of Ni particle, is taken into account by assuming a field-dependent gap $\Delta(B)$. $\Delta(0)$ is calculated from the measured transition temperature T_c of the superconductor, so we have three free parameters to fit the temperature dependence: Z, the effective field B, and the polarization P.

Figures 3(b)–3(e) show numerical fits (points) of our experimental data (solid traces) to the normalized resistance (or conductance) predicted by the modified BTK theory, along with the values of the parameters obtained from the fitting procedure. We found that fixing P at zero nearly always gave inferior fits to those performed with P as a free parameter. For the traces shown in Figs. 3(b)–3(d), the Z values are all similar $(0.38<Z<0.50)$, while the best fits are found with $0.21<P<0.30$, in rough agreement with the value, $P_{Ni}\sim 0.23$ found by FS tunneling spectroscopy,[17] but less than that found in recent work on Andreev reflection in FS structures[10]. Our highest resistance sample [Fig. 3(e)] is fit with a higher value of $Z=2.1$, while also yielding a polarization $P=0.28$. We also observe evidence of a finite spin polarization in the differential resistance as a function of dc current, although these data are not discussed here. We note that the Z values obtained are all within the same range, although the interface resistances are clearly different. We shall return to this point later.

In contrast to previous FS experiments, in many of our devices two or more distinct states were seen in the temperature dependence of the interface below T_c [see Fig. 4(a)]; the samples frequently showed switching between these states while the sample temperature was swept. These multiple states were also seen in the magnetic-field dependence of the interface at fixed temperature. Figure 4(b) shows a number of magnetoresistance (MR) traces for both the interface (R_2) and the overlapping Al (R_{Al}), with field sweeps in both positive and negative directions. There is a strong low-field dependence with sharp jumps at $+350$ and -300 G. A MR trace of the Ni ellipse by itself shows standard anisotropic magnetoresistance (AMR) behavior (see Ref. 13), with sharp jumps at exactly the same fields [see Fig. 4(c)]. Since these jumps are due to the switching of the magnetization from positive to negative orientation (and vice versa), it is clear that the interface resistance R_2 is sensitive to the local field generated by the ferromagnet itself. Even with no applied field, the ferromagnet may generate a substantial amount of flux, and should never be assumed to vanish, especially in this geometry. Furthermore, the absence of multiple states in any part of the sample above T_c suggests that the states seen

in the temperature and field dependences of the interface are due to multiple magnetic screening states in the superconductor itself.

The Z parameter in the BTK model is directly related to the transmission of the interface, in that barriers with higher Z's have correspondingly higher resistances. The Z parameter values in our samples range from 0.38 to 2.1, corresponding to a factor of ~ 5 change in the transmission coefficient, while the interface resistances range from 23 Ω to 1.3 MΩ; thus, although the BTK model seems to provide a qualitative description of our data, a quantitative agreement is lacking. Given the assumptions of the BTK model, however, this lack of agreement is not surprising. The BTK model assumes a δ function potential barrier whose strength is characterized by the parameter Z and a normal metal with no impurity scattering, while our materials and interfaces are clearly more in the diffusive limit. Recent work attempted to take diffusive interfaces into account by assuming a distribution of Z values within the BTK model,[18] or within the framework of nonequilibrium Green's function theory.[19] In addition, the effects of charge imbalance in the superconductor,[19] and the effect of spin-polarized transport in the presence of a magnetic field, where the quasiparticle spectrum in the superconductor is Zeeman split, are only beginning to be considered.[20] While these approaches are certainly more sophisticated than our simple approach, qualitatively they predict behavior similar to our experimental results for the temperature dependence. A complete theory of FS transport in diffusive samples will need to include all these effects together.

In summary, our results are in agreement with recent theoretical work, which suggested that superconducting correlations cannot extend into a ferromagnet over distances larger than the exchange length. In addition, we find that our samples switch between different metastable states which exhibit characteristically different behavior. We believe the large changes in resistance seen in previous experiments arise primarily from the FS interface or the superconductor, which were measured in series or in parallel with the ferromagnet. While our results do not completely preclude the existence of a small proximity effect in samples with cleaner FS interface resistances, they show that it is necessary to explicitly eliminate any possible contribution from the superconductor in searching for a proximity effect in a ferromagnet.

We have benefited from discussions with W. Belzig and M. Giroud. This work was supported by the David and Lucile Packard Foundation, and the National Science Foundation through Grant No. DMR-9801982.

[1] V. I. Fal'ko, A. F. Volkov, and C. Lambert, Phys. Rev. B **60**, 15 394 (1999).
[2] R. Seviour, C. J. Lambert, and A. F. Volkov, Phys. Rev. B **59**, 6031 (1999).
[3] F. Zhou and B. Spivak, cond-mat/9906177 (unpublished).
[4] K. Kawaguchi and M. Sohma, Phys. Rev. B **46**, 14 722 (1992).
[5] J. S. Jiang, D. Davidović, D. H. Reich, and C. L. Chien, Phys. Rev. Lett. **74**, 314 (1995).
[6] M. Giroud, H. Courtois, K. Hasselbach, D. Mailly, and B. Pannetier, Phys. Rev. B **58**, R11872 (1998).
[7] M. D. Lawrence and N. Giordano, J. Phys.: Condens. Matter **11**, 1089 (1999).
[8] V. Petrashov *et al.*, Phys. Rev. Lett. **83**, 3281 (1999).
[9] G. E. Blonder, M. Tinkham, and T. M. Klapwijk, Phys. Rev. B **25**, 4515 (1982).
[10] R. J. Soulen, Jr., J. M. Byers, M. S. Osofsky, B. Nadgorny, T. Ambrose, S. F. Cheng, P. R. Broussard, C. T. Tanaka, J. Nowak, J. S. Moodera, A. Barry, and J. M. D. Coey, Science **282**, 85 (1998).
[11] R. J. Soulen, Jr., M. S. Osofsky, B. Nadgorny, T. Ambrose, P. R. Broussard, S. F. Cheng, J. M. Byers, C. T. Tanaka, J. Nowak, J. S. Moodera, G. Laprade, A. Barry, and J. M. D. Coey, J. Appl. Phys. **85**, 4589 (1999).
[12] We have also measured circular and rectangular elements in similar configurations. Although these results are essentially similar to the elliptical element results, they suffer from nonuniform magnetization distributions in small magnetic fields. For this reason, we concentrate only on elliptical magnets in this paper.
[13] J. Aumentado and V. Chandrasekhar, Appl. Phys. Lett. **74**, 1898 (1999).
[14] To compute the diffusion constants we use ρl values taken from P. Santhanam and D. E. Prober, Phys. Rev. B **29**, 3733 (1984) for Al, and C. Fierz, F.-Z. Lee, J. Bass, W. P. Pratt, Jr., and P. A. Schroeder, J. Phys.: Condens. Matter **2**, 9701 (1990) for Ni. We approximate $v_{F,Ni} \sim 10^8$ cm/s.
[15] P. Charlat, H. Courtois, Ph. Gandit, D. Mailly, A. F. Volkov, and B. Pannetier, Phys. Rev. Lett. **77**, 4950 (1996).
[16] C. Strunk, V. Bruyndoncx, C. van Haesendonck, V. V. Moshchalkov, Y. Bruynseraede, C.-J. Chien, and V. Chandrasekhar, Phys. Rev. B **57**, 10 854 (1998).
[17] R. Meservey and P. M. Tedrow, Phys. Rep. **238**, 173 (1994).
[18] A. A. Golubov, Physica C **327**, 46 (1999).
[19] W. Belzig, A. Brataas, Y. V. Nazarov, and G. E. W. Bauer, Phys. Rev. B **62**, 9726 (2000).
[20] R. Mélin, Europhys. Lett. **51**, 202 (2000).